



Numerical simulations on evaporator coils of sustainable cold storages for food chain application

I.N. Suamir^{a1}, I.M. Rasta^a, A. Winarta^a and I.W. Suirya^a

^aMechanical Engineering Department, Politeknik Negeri Bali, Campus Street Bukit Jimbaran, Kuta Selatan, Bali 80364, Indonesia

Abstract

The development of cold storage in Indonesia is less than satisfactory. As the second highest producers of fishery and aquaculture products in the world, the country has only 2 out of total 6 of its ocean fishing ports possess cold storage facilities. Indonesia is also on the list of low index cold storage markets with abundant natural resources. The lack of cold storage facilities has greatly restricted the development of its fishery and food industries. The current infrastructure is also too poor to exploit the resources efficiently. Under this circumstance, technologies that can encourage development of sustainable cold storages applied for food chain and related components such evaporator coils in the country is in great demand. To date there has not been much research into cold storage evaporator coil design specifically for natural refrigerants such as Hydrocarbon (HC) and CO₂. This paper presents results of theoretical investigation on the main design parameters of natural refrigerant evaporator coils which can be applied in sustainable cold storage systems. The parameters included tube diameter, number of refrigerant circuits, evaporator temperature and circulation ratio. A lumped element technique was applied to develop evaporator models which were used to design and to simulate different coil geometry and circuit arrangements. The results from published papers were used for model validation. The evaporators considered were direct expansion and flooded evaporator coils for low temperature cold storage applications. The paper also presents comparison analyses of natural refrigerant (HC and CO₂) evaporator coils and direct expansion coils using the synthetic refrigerant R-404A.

Keywords: Evaporator coil; natural refrigerants; sustainable cold storage; performance analyses

1. Introduction

Indonesia is an agriculture country with population number of 258.5 million. Poultry, beef and veal production are anticipated to increase 3 to 5 percent annually through 2020, while consumption is expected to rise 4 to 6 percent annually [1]. The country has experienced unbalanced food supply and demand which may need to be well-adjusted through import policy. As an example, beef supply of the country in 2016 was estimated 348,020 tons, while the demand was 651,420 tons [2]. Unbalanced food supply will boost the price of food, sometimes reaching unreasonable level which very much affects the lives of low income populations. This is one of the challenges for the country in improving food security and sustainability.

Furthermore, FAO [3] stated that Indonesia is the second highest producers of fishery and aquaculture products in the world. Fishery and aquaculture production of the country in 2014 was 14.33 million tons. In 2016, the production reached 23.03 million tons which 27.6% came from marine fisheries and 72.4% from aquaculture [4]. Additionally,

Indonesian territory consists of 2/3 of water, has given enormous benefits for Indonesia, especially fishermen. To improve the economic level of fishermen requires efforts to develop proper facilities. One of the efforts is by improving the quality of products which can be marketed in the regional and international levels. It is certainly need the support of the existence of various fishery facilities, one of which is cold storage [5].

The development of cold storage for fishery industry in Indonesia is less than satisfactory. As the second highest producers of fishery and aquaculture products in the world, the country has only 2 out of total 6 of its ocean fishing ports possess cold storage facilities. Moreover, only 4 out of total 14 national fishery ports own cold storage facilities [5]. Indonesia is also on the list of low index cold storage markets with abundant natural resources [1]. The lack of cold storage facilities has greatly restricted the development of its fishery industry. The current infrastructure is also too poor to exploit the resources efficiently. Under this circumstance, technology that can encourage development

¹Corresponding author. Tel.: +6281237594781; Fax: +62361702811
E-mail address: nyomansuamir@pnb.ac.id

Nomenclature

A	Area (m ²)	<i>Greek symbols</i>	
C _p	Specific heat (kJ kg ⁻¹ °C ⁻¹)	δ	
CR	Circulation ratio	η	Thickness
d	Diameter (m)	θ	Efficiency
EC	Evaporator coil	λ	Dry angle
DX	Direct expansion	ρ	Conductivity (kW m ⁻¹ °C ⁻¹)
G	Mass velocity (kg s ⁻¹ m ⁻²)	ω	Density (kg m ⁻³)
H	Enthalpy (kJ kg ⁻¹)	<i>Subscript</i>	Humidity ratio (kg kg _{da} ⁻¹)
j	Colburn j-factor	a	air; air side
h	Heat transfer coefficient (kW m ⁻² °C ⁻¹)	c	convective
LT	Low temperature	cb	convective boiling
MT	Medium temperature	e	evaporator
m	Mass (kg); mass flow rate (kg s ⁻¹)	f	fin
N	Number of rows	i	in; width axis
P	Pressure (kPa)	j	depth axis
Pr	Prandtl number	k	height axis
Q	Refrigeration load (kW)	lat	latent
Re	Reynold number	nb	nucleate boiling
RH	Relative humidity	o	out
S	Suppression factor (m)	r	refrigerant
T	Temperature (°C)	sp	single phase
t	Time (s)	tp	two phase
U	Overall heat transfer coefficient (kW m ⁻² °C ⁻¹)	v	vapor

of infrastructure including cold storage in the country is in extremely great demand.

The demand for refrigerated facilities such as refrigerated warehouse, cold storage and retail refrigeration in Indonesia is expected to increase with the country's economic development because they have a vital role to play in reducing post-harvest losses, improving quantity and quality of fishery and aquaculture products and maintain food supply to consumers. The facilities enable to store over supply of foodstuffs during crop season and use them when there are no crops. The refrigerated facilities are also essential for food quality preservation. However, the increase of refrigerated facilities can provide impact to the environment due to refrigerant leakage and energy use. It has been well-known that refrigeration systems consume intensive energy.

The use of natural refrigerants such as CO₂ and Hydrocarbon offers the opportunity to reduce not only the direct impacts of systems employing HFC refrigerants that possess high global warming potential but also the indirect impacts by improving energy efficiency. Another advantage of CO₂ over HFC refrigerants is its better heat transfer properties that can lead to an increase in the evaporating temperature. A consequence of this is a potential increase in the refrigeration capacity of the coil and a reduction in the rate of frost formation on the coil surface.

Supermarkets have two refrigeration temperature levels, medium temperature (MT) and low temperature (LT) refrigeration. Evaporating temperature of MT refrigeration system is -8°C and -30°C for LT refrigeration system. The refrigeration systems employed can be direct expansion or of the secondary loop type. In conventional supermarkets, the direct expansion refrigeration system is the most commonly used to provide refrigeration to display cabinets

located in the store. For supermarkets which have used natural refrigerants such as CO₂, the applications of secondary refrigeration loops are of particular interest. As CO₂ has low viscosity, the use of CO₂ refrigerant as volatile secondary fluid can significantly improve the performance of the refrigeration system due to its small pumping power. Analyses on secondary loop refrigeration systems using CO₂ as secondary fluid has been reported by [6,7].

Finned tube heat exchangers are commonly used as forced air evaporators of display cabinets in supermarkets. Performance of the evaporator coil directly affects the temperature performance of a display cabinet and the overall performance of the supermarket refrigeration system. The influences of geometry and configuration of finned tube coils using synthetic refrigerants have been intensively investigated by many researchers. Romero-Mendez et al. [8] investigated the effects of fin spacing to the hydrodynamics and heat convection of a plate fin and tube heat exchanger. Liang et al. [9] and Jiang et al. [10] showed the impacts of circuiting on performance and parameter distributions within the tubes and across the coil. Getu and Bansal [11] developed a model of R-404A evaporator coil to analyze the performance of the coils in LT supermarket display cabinets. Chandrasekharan and Bullard [12] developed a design tool for a fin and tube display cabinet evaporator to predict local and overall effects of frost accumulation.

To date there has not been much research into evaporator coil design specifically for CO₂ refrigerant. Aidoun and Ouzzane [13] established a numerical model to study the effects of circuitry of CO₂ finned tube evaporators and found that it was possible to use longer circuits, thus reducing the number of circuits for a given refrigeration capacity. Authors in [14,15] investigated the impact of the

geometry, tube circuitry and tube diameter on the performance of CO₂ evaporators and showed that by reducing the number of circuits could increase the velocity of refrigerant and reduce the total length of pipe. This study investigated the performance of CO₂ evaporator coils under different geometry, circuitry arrangement and different operating conditions for chilled food and frozen food display cabinets in supermarket applications. Comparison analyses with evaporator coils using R-404A refrigerant were also performed.

Supermarket refrigeration systems using HFC refrigerants are responsible for substantial greenhouse gas emissions from leakage of refrigerant to the ambient and indirect emissions from the electrical power used by the compressors, fans and other ancillary equipment [16]. Direct emissions from refrigerant leakage can sometimes be as high as indirect emissions, and for this reason, legislation at has been aimed at effecting reductions in direct emissions. Another way to significantly reduce or completely eliminate direct emissions is through the use of natural refrigerants, such as hydrocarbons, CO₂ and ammonia. In recent years, considerable research has been carried out on the development and application of supermarket refrigeration systems employing natural refrigerants. Most systems deployed in the field are either trans-critical 'booster' CO₂ systems, cascade all CO₂ systems, or subcritical CO₂ systems cascaded with a hydrocarbon system on the high pressure side for heat rejection [17,18,19].

An interesting approach developed and applied by some supermarket chains involves the use of 'integral' hydrocarbon cabinets with heat rejection to the air in the supermarket [20] and combination of heat rejection to the air as well as water in a closed loop system [21]. The heat in the water circuit can be either upgraded through a boiler or heat pump and used for domestic hot water and/or space heating, or rejected to the ambient through a dry cooler. This approach can provide energy integration between the refrigeration and space conditioning systems in the store and offers the potential for energy savings if the system is appropriately designed and controlled.

2. Numerical Model Approach

2.1. Numerical models

Three main numerical models were established to investigate the performance of CO₂ and HC evaporator coils under different geometry, circuit arrangement and different operating conditions. The first model was for the investigation of the performance of MT CO₂ flooded evaporator coil. The second model was for the simulation of the performance of CO₂ DX evaporator coils for both chilled and frozen temperature levels. The third model was for HC (R-1270) DX evaporator coil. The additional model was also developed to analyze the coil performance using refrigerant R-404A for comparative analyses. The models can also be used to design the geometry and tube arrangement of evaporator coils for a given refrigeration capacity. The numerical models apply standard plate fin specification from [22] to determine fin and tube pattern, height and width of the coil. The models were developed using the software EES.

To simulate the flooded and DX evaporator coils, some main assumptions were made as follows: steady state flow

conditions; one dimensional flow for refrigerant inside tubes and air across the coil; negligible thermal losses to the environment; uniform temperature and air flow; constant air side convective heat transfer coefficient over the entire coil; intermediate pressure (P_{int}) to be considered as condensing pressure for CO₂ DX evaporator coil, negligible refrigerant pressure drops of less than 2 K saturated temperature equivalent for DX coils [22] and less than 1 K for flooded coils; the same number of tubes in each circuit with the same fraction of total mass flow rate; quasi steady frosting process; maximum pressure drop at air side after frost to be lower than 0.175 kPa.

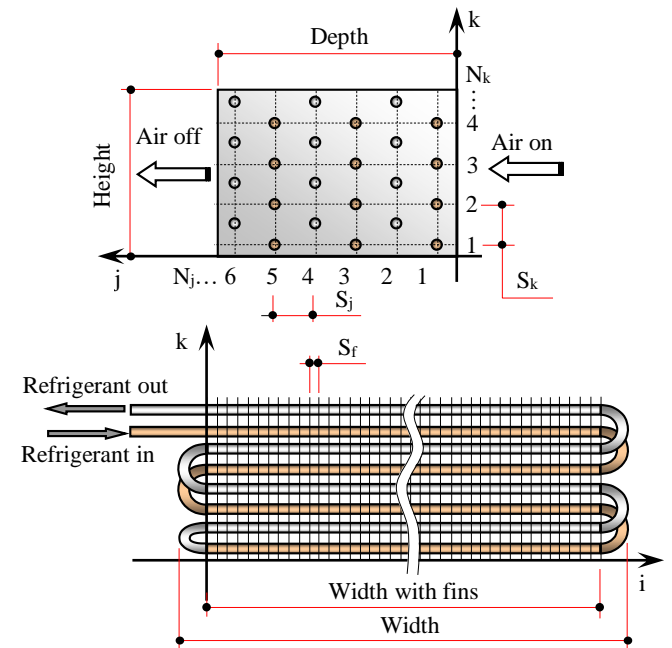


Figure 1. Geometry of a finned tube evaporator model

To simulate the geometry and circuitry of the evaporator coils, certain assumptions were made as follows: constant air side convective heat transfer coefficient over the entire coil; condensing pressure of 12.7 bar_a (corresponds to 29 °C condensing temperature), evaporating temperature of -7 °C; negligible refrigerant pressure drop of less than 2 K saturated temperature drop equivalent; the same number of tubes in each circuit with the same fraction of total mass flow rate; quasi steady frosting process; maximum pressure drop at air side after frost to be lower than 0.175 kPa.

The mathematical modeling approach and design strategy for the coil followed the process described by [15]. The evaporation heat transfer coefficient for refrigerant R1270 was determined from the correlation by [23]. The two phase pressure drop was calculated from [24,25]. The heat transfer coefficient and pressure drop correlations were associated with the flow pattern map developed by [26].

Figure 1 shows the basic geometry of the finned tube evaporator considered in the models. The tubes are arranged in coordinates along width, depth and height axes (i, j, k) as can be seen in the figure. The number of rows and tube pattern can be used to determine the size of the coil and the tube interconnections within the coil circuits. If the coil has more than one circuit, the number of tubes in each circuit should be evenly balanced.

The mathematical models used the lumped element technique by which the evaporator coil can be divided into

the superheated and two phase regions. A DX coil has two lumped regions (single and two phase regions), while a flooded evaporator coil only has a one region, the two phase region as shown in Figure 2. Each region is considered as a single control volume. The fraction of the coil area in each control volume in a DX coil is calculated in proportion to the amount of heat transfer in each control volume.

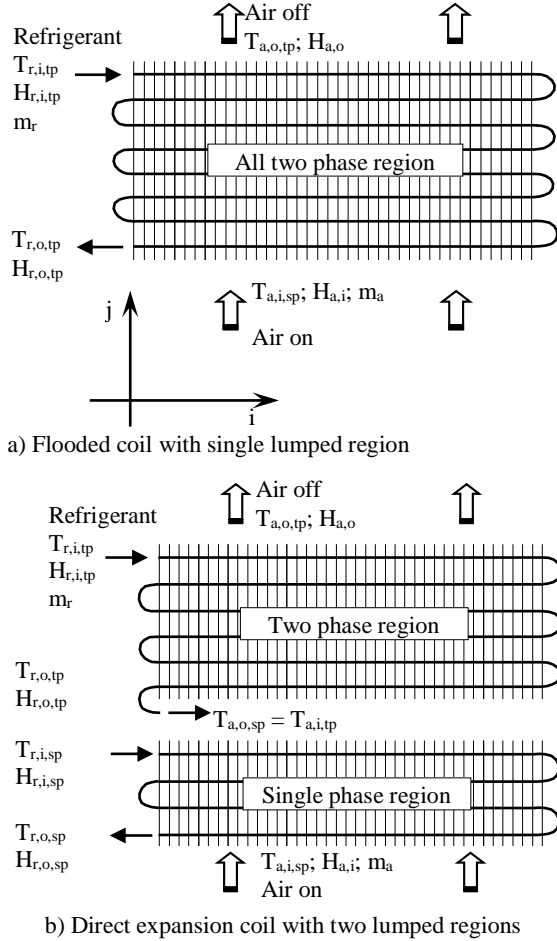


Figure 2. Schematic of flooded and DX evaporator coils with single and two control volumes

The mass and energy balance principles are applied to each control volume, which is summarized in equations (1) to (3). For the flooded evaporator coil, a single phase region does not exist, thus the heat transfer rate component for single phase region ($Q_{r,sp}$) is omitted. ΔT_{lm} is the logarithmic mean temperature difference of each control volume. The air side surface area of the coil (A_a) and other geometric parameters of the coil such as free flow area and free flow area with frost were calculated as in [27].

$$Q_e = Q_{r,tp} + Q_{r,sp} = Q_a \quad (1)$$

$$Q_e = m_r (h_{r,o,tp} - h_{r,i,tp}) + m_r (h_{r,o,sp} - h_{r,i,sp}) = m_a (h_{a,i} - h_{a,o}) \quad (2)$$

$$Q_e = U_{a,tp} A_{a,tp} \Delta T_{lm,tp} + U_{a,sp} A_{a,sp} \Delta T_{lm,sp} \quad (3)$$

The overall heat transfer coefficient (U_a) of the coil with frost can be calculated from equation (4). For frost free coil the component of frost resistance is not included. For the DX coil the external and internal heat transfer areas as well

as the internal heat transfer coefficient depend on the mode of heat transfer, single or two phases.

$$\frac{1}{U_a} = \frac{1}{\eta_f h_a} + \frac{\delta_{frost}}{\eta_f \lambda_{frost}} + \frac{A_a \ln\left(\frac{d_o}{d_i}\right)}{2\pi \lambda_i L_r} + \frac{A_a}{A_r h_r} \quad (4)$$

2.2. Correlations of heat transfer coefficient and pressure drop at refrigerant side

The local heat transfer coefficient and pressure drop for the two phase flow of CO_2 were calculated using the correlations reported by [28,29,30]. The correlations for the two-phase frictional pressure drop for CO_2 were based on the correlations proposed by [24,25].

The local heat transfer coefficients and pressure drop correlations were selected for each flow regime as it changes with the flow and evaporation of refrigerant in the evaporator. Thus the correlations reliably capture the variation of two phase heat transfer coefficient and frictional pressure drops at different mass velocities and vapor qualities.

Equations (5) and (6) show the general equations for the two phase heat transfer coefficient and pressure drop on the refrigerant side of the evaporator. The detailed correlations for each flow regime and for the single phase region can be found in [29,30].

$$h_{tp} = \frac{\theta_{dry} h_v + (2\pi - \theta_{dry}) [(Sh_{nb})^3 + h_{cb}^3]^{(1/3)}}{2\pi} \quad (5)$$

$$\Delta P_{total} = \Delta P_{static} + \Delta P_{momentum} + \Delta P_{frictional} \quad (6)$$

The evaporation heat transfer coefficient for refrigerant R-404A was determined from the correlation by [23]. The two phase pressure drop was calculated from [24,25]. The heat transfer coefficient and pressure drop correlations were associated with the flow pattern map developed by [26].

2.3. Correlations of heat transfer coefficient and pressure drop on the air side

Air side convective heat transfer coefficient has been calculated using the Colburn j-factor proposed by [31], while the total heat transfer coefficient for wet coil and pressure drop were calculated based on the equations by [11]. The air side heat transfer coefficient can be calculated from:

$$h_a = h_{c,a} + h_{at,a} \quad (7)$$

$$h_{c,a} = \frac{j C p_a G_a}{Pr^{2/3}} \quad (8)$$

2.4. Calculation of frost accumulation

Frost accumulation on the evaporator surface has been estimated using the method proposed by [11]. The rate of frost accumulation was determined from equation (9) and the amount of frost accumulated on the surface of the evaporator and frost thickness after Δt time, from equation (10).

$$m_{frost} = m_a (\omega_i - \omega_o) \quad (9)$$

$$\Delta m_{frost} = m_{frost} \Delta t \quad \text{and} \quad \delta_{frost} = \frac{\Delta m_{frost}}{\rho_{frost} A_a} \quad (10)$$

Detailed calculations of density, thermal conductivity and diffusivity of the frost can be found in [11].

3. Results and Discussion

Test results from the experimental CO₂ test facility were used to validate the models. The model of conventional evaporator coil with R-404A was validated against data provided by the manufacturer. Comparison between predictions and experiments under design conditions was found to be satisfactory for the refrigeration capacity as shown in Table 1. The pressure drop estimations were, however, lower than the experiment results mainly because the pressure drops across the distributor and lead tubes were not included in the model. For synthetic refrigerants these pressure drops can be as high as 89% of total pressure drops in the evaporator coil [32].

The validated models were used to design 8 evaporator coils with different geometry and circuitry. The evaporator coils were simulated at evaporating temperature of -8 °C for MT coils and -30 °C for LT coils. Tubes and fins were made from copper and aluminum respectively. Equilateral fin and tube pattern in a staggered arrangement was applied. The temperature of chilled food display cabinet was in the range of -1 to 1 °C and frozen food display cabinet was in the range of -19 to -21 °C.

Table 1. Numerical model and experimental results

Parameters		a) MT CO ₂ Models		b) DX LT CO ₂ model	c) DX R-404A model
		Flooded	DX		
Q _e (kW) full load, ΔT _a = 10 K	Model/Experiment	5.19 5.10	5.09 4.93	3.00 2.89	- -
Q _e (kW) steady state load, ΔT _a = 9 K for MT and ΔT _a = 8 K for LT	Model/Experiment	4.55 4.42	4.46 4.30	2.35 2.12	3.65 3.60*
ΔP _r (kPa) steady state	Model/Experiment	11.31 21.15	9.22 16.87	6.01 14.87	40.92 148.28*

Evaporator coil investigated:

a) Tube arrangement: staggered; d_o = 12.70 (mm); N_k = 4; N_j = 6; number of circuits = 4; fins pitch 4 fins/inch

b) Tube arrangement: staggered; d_o = 12.70 (mm); N_k = 4; N_j = 8; number of circuits = 3; fins pitch 3 fins/inch

c) Tube arrangement: inline; d_o = 15.87 (mm); N_k = 2; N_j = 16; number of circuits = 2; fins pitch 3 fins/inch

* Data from manufacturer

Table 2 shows the geometry of the evaporator coils together with their performance parameters. It can be seen the physical sizes of the CO₂ evaporator coils are varied and are generally much smaller compared to the coils with R-404A. For the given refrigeration duty, the flooded MT coil with tube diameter 9.52 mm (EC-3) has the smallest size with refrigerant volume about 62% of the MT DX coil using the same tube diameter (EC-1) and about 19% of that in the R-404A evaporator coil (EC-5).

Table 2. Geometry of the designed coils with their performance parameters

Parameters	MT evaporator coils					LT evaporator coils		
	DX CO ₂		Flooded CO ₂		DX R-404A	DX CO ₂		DX R-404A
	EC-1	EC-2	EC-3	EC-4	EC-5	EC-6	EC-7	EC-8
Tube outside diameter (mm)	9.52	12.70	9.52	12.70	15.87	9.52	12.70	15.87
Number of rows high	2	2	2	2	2	2	2	2
Number of rows deep	21	17	13	10	20	12	10	12
Number of circuits	2	1	2	1	2	2	1	2
Total tube length (m)	91.1	73.8	56.4	43.4	86.6	48.7	40.6	48.7
Height (mm)	63.5	63.5	63.5	63.5	76.2	63.5	63.5	76.2
Depth (mm)	577.4	467.4	357.5	275.0	659.9	330.0	275.0	395.9
Width with fins (mm)	2170	2170	2170	2170	2170	2030	2030	2030
Refrigerant volume (L)	4.14	6.78	2.56	3.99	13.47	2.22	3.74	7.57
G _r (kg s ⁻¹ m ⁻²)	171.0	168.7	199.8	198.1	109.0	100.4	99.0	72.2
CR	-	-	1.2	1.2	-	-	-	-
Q _e (kW)	3.75	3.75	3.75	3.76	3.76	2.25	2.25	2.25
Q _{e,frost} (kW)*	3.26	3.12	3.24	2.96	3.44	2.16	2.14	2.15
Fin efficiency	0.85	0.88	0.85	0.88	0.87	0.89	0.92	0.90
h _r (kW m ⁻² °C ⁻¹)	2.899	3.107	3.206	3.473	0.482	2.521	2.802	0.337
h _a (kW m ⁻² °C ⁻¹)	0.062	0.073	0.064	0.075	0.063	0.042	0.050	0.046
ΔP _r (kPa)	65.13	30.89	42.34	19.27	50.47	33.15	16.24	31.79
ΔP _{a,frost} (kPa)	0.016	0.024	0.030	0.043	0.013	0.018	0.020	0.010

The CO₂ coils also need less refrigerant charge as shown in Fig. 3, assuming 25% and 35% of the evaporator volume was filled with liquid for the DX and flooded evaporator coils respectively.

The CO₂ evaporator coils with smaller tube diameter require more tube rows and longer tubes to meet the designed refrigeration duty. Using single circuit arrangement results in high pressure drop particularly for the DX type coils. As can be seen in Table II the pressure drops of the CO₂ coils (EC-1, EC-3 and EC-6) are still higher than the coils with larger tube diameter (EC-2, EC-4 and EC-7) even in two circuit arrangement. The pressure

drop will be higher if the pressure drop across the distributor and lead tubes is taken into account. Moreover, the physical size of the coils, except for in the case of the flooded coil EC-3, is larger which may increase their production cost.

Figure 4 shows the performance variation of CO₂ MT DX coils with evaporating temperature. Increasing the evaporating temperature can slightly improve the refrigeration capacity and reduce the pressure drop. Similar effect was also found on the LT DX and flooded evaporator coils. In Figures 5 and 6, the performance of the flooded CO₂ evaporator coils at different circulation ratios (CR) is shown.

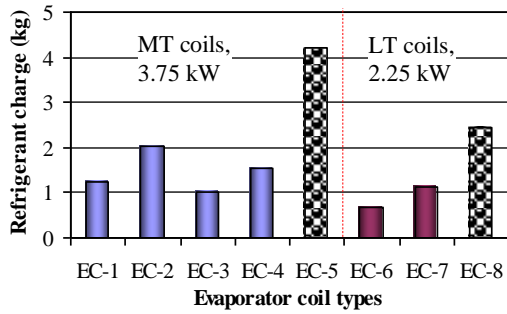


Figure 3. Refrigerant charge comparisons

As the CR increases, the refrigeration duty slightly improves due to the enhancement of the evaporation heat transfer coefficient. However, the increase of the CR considerably increases the pressure drop and refrigerant mass velocity which increases the power consumption of the CO₂ pump and causes a reduction in the coefficient of performance of the refrigeration system. The CR, therefore, should be chosen to be as low as possible in the range of the designed refrigeration capacity. The experimental tests showed the optimum CR to be in the range 1.1 and 1.3.

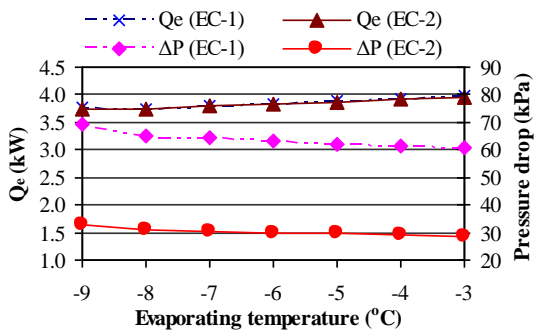


Figure 4. The influence of evaporating temperature

Numerical models have been developed and validated for design and performance simulation of finned tube flooded and direct expansion coils. Different geometry and circuitry arrangements were simulated using CO₂ and R-404A as refrigerants. The investigation found that for a given refrigeration capacity, CO₂ evaporator coils had considerably smaller size and lower refrigerant charge compared to the coils using R-404A refrigerant.

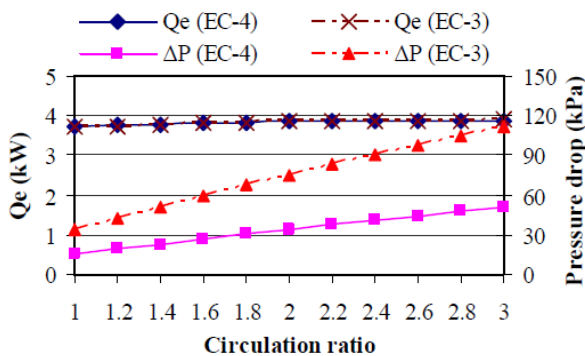


Figure 5. Refrigeration duty and pressure drops with circulation ratio (CR)

The investigation among the CO₂ evaporator coils showed that for the refrigeration capacity examined, using the larger tube diameter, the CO₂ DX evaporator coils were found to be more compact due to smaller number of rows along the depth of the coil. The pressure drop of the coils was also found to be lower. However, the coil had more refrigerant charge compared to the coil with the smaller tube diameter. For the CO₂ flooded evaporator application, the use of smaller tube diameter was found to be more favorable in terms of coil size and refrigerant charge.

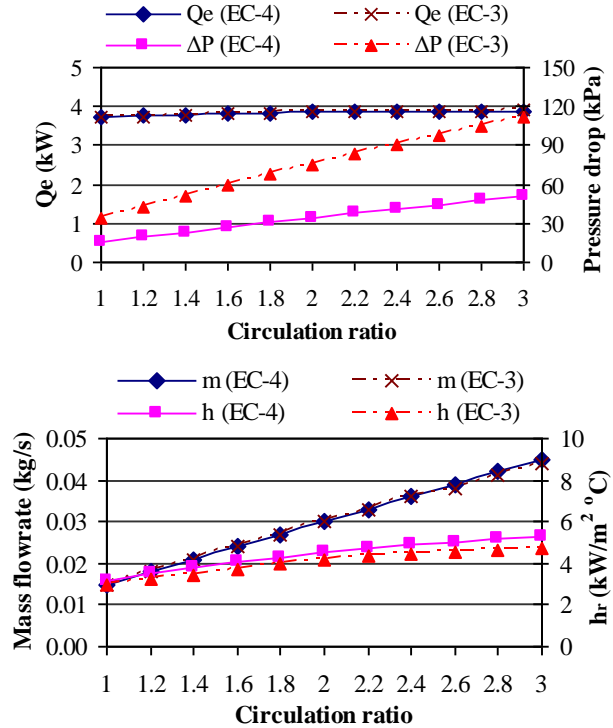


Figure 6. Refrigerant mass flow rate and heat transfer coefficient with circulation ratio

Table 3. Geometry of the designed coil with its performance parameters

Parameters	R1270 coil	R404A coil
Tube outside diameter (mm)	12	12
Number of rows high	2	2
Number of rows deep	10	14
Number of circuits	2	2
Total tube length (m)	70	98
Height (mm)	70	70
Depth (mm)	350	490
Width with fins (mm)	3500	3500
Refrigerant volume (L)	7.1	7.8
Refrigerant charge (kg)+	0.640	2.438
G _r (kg s ⁻¹ m ⁻²)	67.66	206.1
Q _e (kW)	4.2	4.2
Q _{e,frost} (kW)*	3.4	3.6
Fin efficiency**	0.83	0.84
h _r (kW m ⁻² °C ⁻¹)	0.738	1.318
h _a (kW m ⁻² °C ⁻¹)	0.052	0.048
ΔP _r (kPa)	8.53	97.38
ΔP _{a,frost} (kPa)*	0.016	0.010

* After frost accumulation of 240 minutes

**Fin thickness: 0.2 (mm); Fin pitch: 8 (mm) for R1270 and 10 (mm) for R404A

+ Assumption 25% of the coil volume filled with liquid refrigerant.

Table 3 details the geometry of the R-1270 evaporator and original R-404A coil together with performance parameters obtained from the EES model. Because the R-1270 refrigeration system is comprised of two circuits, the coil geometry given in the table is for only one circuit. Similar assumptions were made for the R-404A coil. A 7 °C superheat was also assumed for both coils. The results show that for the same load the R-1270 coil would require 70 m of copper pipe and 0.64 kg of refrigerant charge compared to 98 m pipe for the R-404A coil and 2.44 kg of refrigerant charge.

4. Conclusions

Numerical models have been developed and validated for design and performance simulation of finned tube flooded and direct expansion coils which can be applied in sustainable cold storage systems. Different geometry and circuitry arrangements were simulated using natural refrigerant CO₂ and Hydrocarbon (HC). For comparison simulation also performed for R-404A evaporator.

The investigation found that for a given refrigeration capacity, CO₂ evaporator coils had considerably smaller size and lower refrigerant charge compared to the coils using R-404A refrigerant. The investigation among the CO₂ evaporator coils showed that for the refrigeration capacity examined, using the larger tube diameter, the CO₂ DX evaporator coils were found to be more compact due to smaller number of rows along the depth of the coil.

The pressure drop of the coils was also found to be lower. However, the coil had more refrigerant charge compared to the coil with the smaller tube diameter. For HC evaporator coil, the results showed that, at the same refrigeration load, the HC coil would require 40% shorter copper pipe and 30% refrigerant charge compared to R404A evaporator coil.

Acknowledgment

The authors acknowledge the financial support received from the Higher Education Directorate General of the Ministry of Education and Culture of the Republic of Indonesia.

References

- [1] J. Miller, "Top Markets Report Cold Chain, International Trade Administration," 2016, available from: http://trade.gov/topmarkets/pdfCold_Chain_Executive_Summary.pdf
- [2] BPS, "Peternakan dalam angka-2016. Badan Pusat Statistik (Statistics Indonesia)," Jakarta, 2016, p. 101
- [3] FAO, "The State of World Fisheries and Aquaculture 2016. Contributing to food security and nutrition for all," Rome, 2016, p. 200.
- [4] MMAF-RI, "Capture and aquaculture production 2012-2016. Ministry of Marine Affairs and Fisheries Republic of Indonesia," 2016, available from: <http://statistik.kkp.go.id/sidatik-dev/2.php?x=2>
- [5] I.M. Putri and D.R. Munaf, "Increasing fishery economic added value through post fishing program: Cold storage program," International Journal of Social, Behavioral, Educational, Economic, Business and Industrial Engineering, 7, 2013, pp. 2391-2394
- [6] S.W. Inlow and E.A. Groll, "Analysis of secondary loop refrigeration systems using carbon dioxide as volatile secondary refrigerant," HVAC&R Research, 2, 1996, pp. 107-120.
- [7] A. Melinder and E. Granryd, "What to consider when using secondary fluids in indirect systems, Proc. Sustainable Refrigeration and Heat Pump Conference, Sweden, 2010, p. 12
- [8] R. Romero-Mendez, M. Sen, K.T. Yang, R. McClain, "Effect of fin spacing on convection in plate fin and tube heat exchanger," Int. J. Heat and Mass Transfer, 43, 2000, pp. 39-51.
- [9] S.Y. Liang, T.N. Wong, G.K. Nathan, "Numerical and experimental studies of refrigerant circuitry of evaporator coils," Int. J. Refrig., 24, 2001, pp. 823-833.
- [10] H. Jiang, V. Aute, R. Radermacher, "Coil designer: a general-purpose simulation and design tool for air-to-refrigerant heat exchangers," Int. J. Refrig., 29, 2006, pp. 601-610.
- [11] H.M. Getu and P.K. Bansal, "Modelling and performance analyses of evaporators in frozen-food supermarket display cabinets at low temperatures," Int. J. Refrig., 30, 2007, pp. 1227-1243.
- [12] R. Chandrasekharan, P. Verma, C.W. Bullard, "Development of a design tool for display case evaporators," Int. J. Refrig., 29, 2006, pp. 823-832.
- [13] Z. Aidoun and M. Ouzzane, "A model application to study circuiting and operation in CO₂ refrigeration coils," Appl. Therm. Eng., 29, 2009, pp. 2544-2553.
- [14] J.A. Shilliday and S.A. Tassou, "Numerical analysis of a plate fin and tube evaporator using the natural refrigerant CO₂," Proc. 1st IIR International cold chain conference, Sustainability and the Cold Chain, Cambridge, 2010.
- [15] I.N. Suamir and S.A. Tassou, "Modeling and performance analyses of CO₂ evaporator coils for chilled and frozen food display cabinets in supermarket applications," Proc. International Congress of Refrigeration, Prague, 2011, p. 8.
- [16] S.A. Tassou, J.S. Lewis, Y.T. Ge, A. Hadaway, I. Chaer, "A review of emerging technologies for food refrigeration applications," Appl. Therm. Eng., 30, 2010, pp. 263-276.
- [17] S. Giroto, S. Minetto, P. Neksa, "Commercial refrigeration system using CO₂ as the refrigerant," Int. J. Refrig., 27, 2004, pp. 717-723.
- [18] A. Campbell, G.G. Maidment, J.F. Missenden, "A natural refrigeration system for supermarkets using CO₂ as a refrigerant," Proc. CIBSE National Conference, London, 2006.
- [19] D. Hinde, S. Shitong Zha, L. Lan, "Carbon dioxide in North American supermarkets," ASHRAE Journal, 51, 2009, pp. 18-26.
- [20] Lidl, "Two hundred Lidl stores to feature R290 technology by 2012, 2011, available from: <http://www.hydrocarbons21.com/content/articles/2011-01-14-200-lidl-stores-to-feature-r290-technology-by-2012.php>.

- [21] J. Gartshore, and S. Benton, "Cool concerns and Waitrose to support the use of hydrocarbons," 2010, available from: <http://www.hydrocarbons21.com/content/articles/2010-07-22-cool-concerns-and-waitrose-to-support-the-use-of-hydrocarbons.php>.
- [22] SRC, "Standard plate fin coil specifications," 2010, available from: http://www.srcoils.com/wp-content/blogs.dir/1/files/2010/05/Coil_Specs_Nomenclature.pdf
- [23] L. Wojtan, T. Ursenbacher, J.R. Thome, "Investigation of flow boiling in horizontal tubes: Part II-Development of a new heat transfer model for stratified-wavy, dryout and mist flow regimes," *Int. J. Heat and Mass Transfer*, 48, 2005b, pp. 2970-2985.
- [24] J. Moreno Quiben, J.R. Thome, "Flow pattern based two-phase frictional pressure drop model for horizontal tubes. Part I: Diabatic and adiabatic experimental study," *Int. J. Heat and Fluid Flow*, 28, 2007a, pp. 1049-1059.
- [25] J. Moreno Quiben, J.R. Thome, "Flow pattern based two-phase frictional pressure drop model for horizontal tubes. Part II: New phenomenological model," *Int. J. Heat and Fluid Flow*, 28, 2007b, pp. 1060-1072.
- [26] L. Wojtan, T. Ursenbacher, J.R. Thome, "Investigation of flow boiling in horizontal tubes: Part I-A new diabatic two-phase flow pattern map," *Int. J. Heat and Mass Transfer*, 48, 2005a, pp. 2955-2969.
- [27] R.K. Shah, D.P. Seculic, "Fundamental of heat exchanger design, John Wiley & Sons Inc., New Jersey, 2003, pp. 564-574.
- [28] L. Cheng, G. Ribatski, L. Wojtan, J.R. Thome," New flow boiling heat transfer model and flow pattern map for carbon dioxide evaporating inside horizontal tubes," *Int. J. Heat and Mass Transfer*, 49, 2006, pp. 4082-4094.
- [29] L. Cheng, G. Ribatski, J. Moreno Quiben, J.R. Thome, 2008, New prediction methods for CO₂ evaporation inside tubes: Part I - A two-phase flow pattern map and a flow pattern based phenomenological model for two-phase flow frictional pressure drops," *Int. J. Heat and Mass Transfer*, 51, 2008, pp. 111-124.
- [30] L. Cheng, G. Ribatski, J.R. Thome, "New prediction methods for CO₂ evaporation inside tubes: Part II -An updated general flow boiling heat transfer model based on flow patterns," *Int. J. Heat and Mass Transfer*, 51, 2008, pp.125-135.
- [31] N.H. Kim, B. Youn, R.L. Webb, "Air side heat transfer and friction correlations for plain fin and tube HX with staggered tube arrangements, *J. Heat Transfer Transactions of the ASME*, 1999, pp. 662-667.
- [32] SRC, "Refrigerant evaporator (DX) coil," 2001, available from: <http://www.srcoils.com/File/PDF/Evap%20Coil%20Primer.pdf>